Temperature and frequency dependence of anelasticity in a nickel oscillator

Robert F. Berg

Thermophysics Division, Chemical Science and Technology Laboratory, National Institute of Standards and Technology, Gaithersburg, Maryland 20899

The frequency dependence of the real and imaginary parts of a nickel oscillator's transfer function is described over 3 decades in frequency by the use of simple expressions. These expressions incorporate only the resonance frequency ω_0, the quality factor Q, and a characteristic exponent β determined by a single measurement of creep. They are based on the ansatz $\phi(\omega) = Q^{-1}(\omega/\omega_0)^{-\beta}$, where ϕ is the imaginary part of the spring constant. Over a 100 K range of temperature T, the exponent $\beta \simeq 0.18$ was constant even though $Q(T)$ changed by a factor of 8. These expressions are potentially useful for accurately describing a mechanical oscillator whose transfer function must be modeled at frequencies far below ω_0. Examples include accelerometers based on a flexure element and suspensions for interferometric gravitational wave detectors.

I. INTRODUCTION

Anelasticity,[1-3] the complex generalization of elasticity, is required to describe a mechanical oscillator incorporating a solid elastic element over a wide span of frequency. One example of such an oscillator is an accelerometer consisting of a proof mass suspended by a flexure element and operated far below its resonance frequency. Because anelasticity is a linear property of the solid, anelastic creep (see, e.g., Ref. 4) can be significant even at strains far below the flexure's elastic limit. A second example is the flexure element of a balance used for comparison of reference masses.[5] A third example is the suspension system needed for the mirrors of a gravitational wave detector. Although the suspension system is needed to reduce seismic noise, its thermally driven noise increases with its internal loss. Thus, knowledge of the oscillator's loss as a function of frequency is required to predict the instrument's noise spectrum, especially at low frequencies.[6] Gillispie and Raab[7] used anelasticity to interpret suspension losses measured in a prototype of the Laser Interferometric Gravitational-Wave Observatory (LIGO).[8] The instrument which motivated the present study is a viscometer which consists of a nickel oscillator immersed in the fluid whose viscosity is to be measured.[9] The viscometer's calibration required an accurate characterization in vacuum from 0.001 to 12 Hz.

The nickel oscillator was characterized by first measuring the resonance frequency ω_0 and quality factor Q in vacuum. Then the oscillator's response to a harmonic force, or the transfer function $H(\omega)$, was measured at low frequencies ω. The expected result was

$$H(\omega) \equiv \frac{x(\omega)}{F(\omega)} = [-m\omega^2 + im\omega_0 Q^{-1}\omega + k]^{-1}, \qquad (1)$$

where $F(\omega)$ and $x(\omega)$ are the Fourier transforms of the applied force and resulting displacement, and m and k, the oscillator's mass and spring constant, are real and independent of frequency. Instead, as shown in Fig. 1, deviations from Eq. (1) as large as 2% in the magnitude and 0.6° in the phase were found. Similar deviations persisted even when the oscillator was overdamped by immersing it in xenon. Because these deviations were unexpected, they were attributed to anelasticity only after instrumental error was ruled out.

Equation (1), the usual model for a linear oscillator, describes the oscillator's dissipation by a "viscous" term which is proportional to the oscillator's velocity and independent of frequency. The resulting transfer function is a sufficient description of most linear oscillators in a narrow range of frequencies near ω_0. However, for a mechanical oscillator with a solid elastic element, the transfer function's accuracy is improved by removing the viscous term and allowing the oscillator's spring constant k to be complex, namely

$$H(\omega) = \{-m\omega^2 + k(\omega)[1 + i\phi(\omega)]\}^{-1}. \qquad (2)$$

Saulson[6] emphasized the superiority of Eq. (2) for accurately modeling the noise spectrum of gravitational wave detectors.

The usual and simplest assumption is that ϕ is independent of frequency. [The causality requirement that $\phi(\omega)$ be odd in ω is not a restriction at $\omega \neq 0$.] This is a good approximation for some materials over a wide range of frequencies.[5,10] However, in general there are many microscopic dissipation mechanisms, each of which can contribute its own frequency dependence to ϕ. Indeed, the dependences of ϕ on frequency and temperature are used as probes of material microstructure, and conferences on internal friction are held every few years.[11,12] In contrast to polymer science, where measurements of complex viscosity have a long history,[13] most studies of complex elastic moduli in crystalline materials have been measurements of ϕ's temperature dependence at constant frequency. More recently, several groups[14-17] have developed devices which measure the frequency dependence of ϕ over many decades below the instrument's resonance frequency. Rivière and Woirgard[18] found an extreme example of such frequency dependence: in a glass–ceramic matrix reinforced by SiC fibers, ϕ increased 10 times when the frequency was changed by a factor of 10.
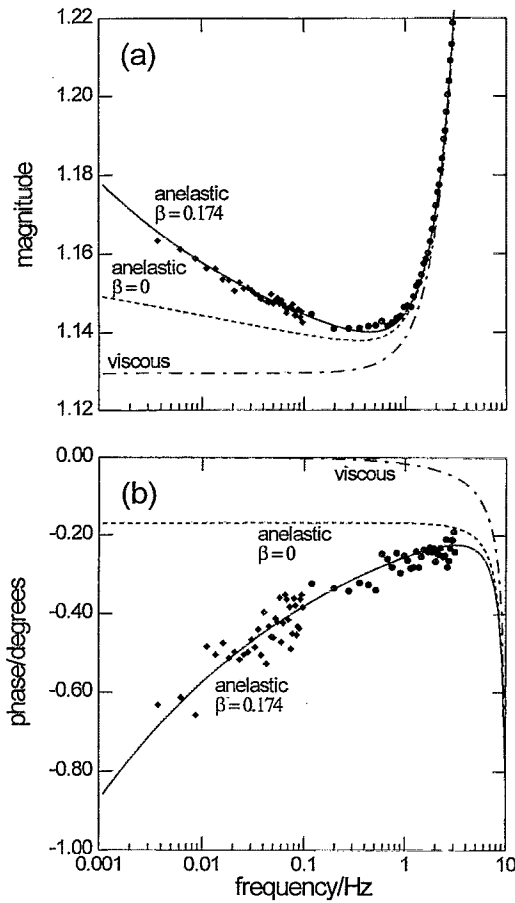
FIG. 1. The transfer function $H(\omega)$ for oscillator D at 61 °C measured at low frequencies. The original data, spaced linearly in frequency, were averaged in groups of 10. The different symbols distinguish data taken in two different frequency ranges of the spectrum analyzer. (a) The measured magnitude $k_{tr}|H(\omega)|$. Anelasticity increases the spring's compliance, and thus $|H(\omega)|$, at low frequencies. The "viscous" curve from Eq. (1) and the "anelastic" curve with $\beta=0$ are inadequate to describe the data. (b) The phase of $H(\omega)$. The anelastic loss prevents the phase from approaching zero, even near 1 mHz.

The temperature dependence of ϕ can also be large. For example, Buck et al.[19] measured an order-of-magnitude increase of ϕ within a temperature span of only 30 K in oxygen-doped V–Nb alloys.

The purpose of this paper is to make two suggestions that are useful when ϕ's frequency dependence is weak. First, a simple functional form for $\phi(\omega)$ is proposed. Second, the Kramers–Kronig integrals[2] which relate the imaginary part of the oscillator's spring constant to its real part and to its creep behavior are rewritten in terms of the oscillator's properties at $\omega=\omega_0$ instead of the unattainable frequencies $\omega=0$ or $\omega=\infty$. Thus, the oscillator can be characterized at frequencies far below ω_0 by measurements near ω_0 plus a single measurement of creep.

In the following, the imaginary part of the oscillator's spring constant is approximated by the simple function

$$\phi(\omega)=Q^{-1}\left(\frac{\omega}{\omega_0}\right)^{-\beta}. \tag{3}$$

Before measurements of ϕ's frequency dependence were common, Schoeck et al.[20] considered the possibility of a power-law dependence of ϕ. Recently, such frequency dependence has been seen in a pure metal,[21] an alloy,[22] and a ceramic.[23] In particular, Rivière and Woirgard[21] measured the internal friction of strain-hardened aluminum. Replotting their data on a logarithmic scale shows that $\phi(\omega)$ was approximately proportional to $\omega^{-\beta}$ with $\beta\approx0.28$ over the range from 10^{-3} to 1 Hz in the temperature range from 90 to 216 °C.

Equation (3) is consistent with an underlying scale-invariant distribution of time constants in the solid element. However, demonstration of such a distribution's existence is unnecessary for Eq. (3) to be useful, and Eq. (3) describes the present oscillator's behavior with a single temperature-independent exponent β and the easily measured quantities $Q^{-1}(T)$ and $\omega_0(T)$.

In Sec. II, Eq. (3) for $\phi(\omega)$ will be inserted into appropriate integrals to yield Eq. (10) for the real part of the oscillator's spring constant and Eq. (14) for the time dependence in a creep experiment. The simplicity of these expressions suggests their use for practical models of mechanical oscillators. As demonstrated by the present oscillator, the applicable ranges of frequency and temperature can be broad. Measurements of $\omega_0(T)$ and $Q(T)$ and a single measurement of creep provided sufficient information to describe the oscillator's transfer function over more than 3 decades of frequency below ω_0 and over a 100 K temperature range in which $Q(T)$ varied by a factor of 8.

II. THE ANELASTIC SPRING

Because the imaginary and real parts of the spring constant are connected by a Kramers–Kronig relation, k in Eq. (2) must depend on frequency. Therefore, it is useful to separate out explicitly all of k's frequency dependence by the definition

$$k(\omega)[1+i\phi(\omega)]\equiv k_0[1+\psi(\omega)+i\phi(\omega)], \tag{4}$$

so that the transfer function is

$$H(\omega)=k_0^{-1}\left[1-\left(\frac{\omega}{\omega_0}\right)^2+\psi(\omega)+i\phi(\omega)\right]^{-1}. \tag{5}$$

By defining $k_0\equiv\mathrm{Re}[k(\omega_0)]$ and using $\omega_0^2=k_0/m$, the quantities m and Q do not appear in Eq. (5). This is equivalent to the conditions at resonance of

$$\psi(\omega_0)\equiv0; \quad \phi(\omega_0)=Q^{-1}. \tag{6}$$

The creep displacement $x(t)$ following a step change in the applied force is proportional to the spring material's time-dependent compliance $J(t)$. This compliance, which depends on the strain history, is usually characterized by its Fourier transform $J_1(\omega)-iJ_2(\omega)$.

If ψ and ϕ are much less than 1, they can be written in terms of the compliances J_1 and J_2 as

$$\psi(\omega)\cong\frac{J_1(\omega_0)-J_1(\omega)}{J_1(\omega_0)} \tag{7}$$

and

$$\phi(\omega) \cong \frac{J_2(\omega)}{J_1(\omega_0)}. \tag{8}$$

Substitution of the Kramers–Kronig relation into Eq. (7) gives the real part $\psi(\omega)$ in terms of the imaginary compliance $J_2(\omega)$:

$$\psi(\omega) = \frac{(2/\pi)}{J_1(\omega_0)} \int_0^\infty \frac{J_2(\omega_1)\omega_1}{(\omega_1^2 - \omega_0^2)} - \frac{J_2(\omega_1)\omega_1}{(\omega_1^2 - \omega^2)} d\omega_1. \tag{9}$$

Use of Eq. (8) and the simple form of Eq. (3) for $\phi(\omega)$ then gives

$$\psi(\omega) = \frac{Q^{-1}[1 - (\omega/\omega_0)^{-\beta}]}{\tan(\pi\beta/2)}. \tag{10}$$

Equation (10) requires the oscillator's spring to be weaker at lower frequencies. This is true even for frequency-independent ϕ, corresponding to $\beta=0$, in which case

$$\psi(\omega, \beta \equiv 0) = (2/\pi)Q^{-1} \ln(\omega/\omega_0). \tag{11}$$

The time-dependent compliance $J(t)$ also can be estimated from knowledge of only the oscillator's dissipation. Nowick and Berry[2] quote the result

$$\frac{dJ(t)}{dt} = \left(\frac{2}{\pi}\right) \int_0^\infty J_2(\omega)\sin(\omega t)d\omega. \tag{12}$$

Again using the expression for $\phi(\omega)$ and integrating with respect to time, one obtains

$$\frac{J(t) - J(0)}{J_1(\omega_0)} = \frac{2Q^{-1}\Gamma(1-\beta)}{\pi\beta} \cos(\pi\beta/2)(\omega_0 t)^\beta, \tag{13}$$

so that relaxation (retardation) following a step change in the applied force is not exponential. Although in this expression the initial compliance $J(0)$ is undetermined, it can be estimated by noting that the oscillator's inertia prevents an instantaneous response to the applied force. Thus, $J(0) \cong J_1(\omega_0)$. Then, Eq. (13) becomes

$$x(t) \propto J(t) = J_1(\omega_0)[1 + f(\beta)Q^{-1}(\omega_0 t)^\beta], \tag{14}$$

where

$$f(\beta) \equiv \frac{2\Gamma(1-\beta)}{\pi\beta} \cos(\pi\beta/2). \tag{15}$$

Equation (14) is an example of the "elastic aftereffect,"[2] creep which is due solely to a linear property of the solid.

III. APPARATUS

The 1 mg oscillator was cut from a large piece of nickel screen prepared commercially by electrodeposition.[24] The screen's wires were spaced every 847 μm on a square grid. Electron microscopy showed the cross section of an individual wire to be approximately an 8×30 μm rectangle. The nickel surface was covered by protruding crystals 1 μm in size and smaller. Figure 2 is a schematic diagram of the oscillator. It was constructed by cutting an 8×19 mm rectangle out of the larger screen while leaving two wire extensions to form the torsion fiber.

Four oscillators were made by attaching their torsion fibers to stiff yokes with a Pb–Sn solder. A fifth oscillator was
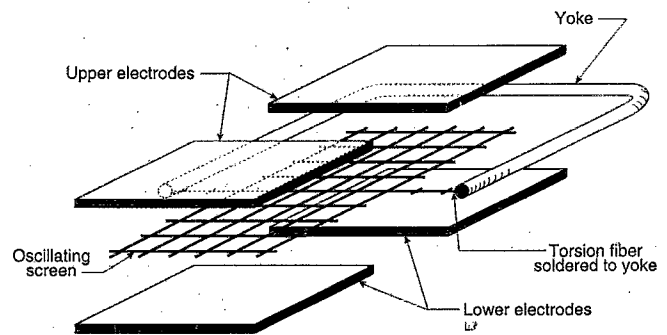

FIG. 2. Schematic diagram of the oscillator. It was constructed by cutting an 8×19 mm rectangle out of a larger nickel screen while leaving two wire extensions to form the torsion fiber. The ends of the torsion fiber were attached to the yoke by the Pb–Sn solder. The oscillator was centered between four fixed electrodes which were connected electrically into diagonally opposite pairs. Oscillating voltages were applied between the electrode pairs and the screen to excite motion of the oscillator.

attached by a silver brazing alloy instead of the Pb–Sn solder. The yoke was centered between four electrodes parallel to the screen, and the complete assembly was sealed into a copper cell. The fixed electrodes were connected electrically into diagonally opposite pairs. Each pair had a total capacitance to the screen of 0.5 pF.

The lowest frequency resonance of the oscillator was the torsion mode at 11 Hz. (The brazed oscillator had thicker wires and thus had a torsion mode at 16 Hz.) The next mode was a flexure about the torsion axis, and it had a resonance above 50 Hz. Due to both the large difference in modal frequencies and the symmetry of the driving electrodes, only the torsion mode was excited.

A commercial spectrum analyzer[25] generated oscillating voltages that were applied between the electrode pairs and the screen in order to move the screen. To make the applied torque proportional to the source voltage, the source voltage was first added to two dc bias voltages of opposite sign. The biased sums were then amplified by square root amplifiers and the resulting voltages were applied to the diagonally opposed electrode pairs.

The oscillating screen and the fixed electrodes also formed a capacitance bridge that was operated at 10 kHz to detect the screen's displacement. The bridge's signal was detected by a lock-in amplifier whose time constant was set at 1 ms. (This time constant was accounted for in the transfer function.) The amplifier's output was linear in the difference between the capacitance of each pair of electrodes and the screen; thus it was a nearly linear function of the screen's displacement.

The spectrum analyzer recorded the source voltage, proportional to $F(t)$, in channel 1, and the capacitance's bridge's error signal, linear in $x(t)$, in channel 2. Harmonic generation and nonlinearity in the entire system, including the drive, the oscillator, and the detection system, was less than 0.2%. Further details may be found in Ref. 9.

IV. PROCEDURE

The four cells containing the soldered oscillators were evacuated and baked at 80–100 °C for 4–8 h. This annealing

increased the Q by a factor of 2 to 3. The brazed oscillator was baked at 80 °C for the much longer time of 70 h.

The oscillator's resonance frequency ω_0 and Q were obtained by fitting to the transfer function measured in a narrow interval, typically 0.8 Hz, centered on ω_0. The spectrum analyzer was set up for a "random" excitation signal, continuous triggering, and a Hanning filter function. After acquiring data for 30 min, ω_0 and Q could be determined to within 0.01% and 10%, respectively. The Q measured in this manner agreed with that calculated from observations of the free decay of the oscillator's amplitude. The drive amplitude was chosen to limit oscillator motion to 1 mrad.

Drag caused by residual gas in the cell was estimated from kinetic theory and ruled out as a significant contribution to Q^{-1}. The pressure used in this calculation was that measured at the vacuum pump. Although outgassing raised the cell's pressure above the pump's pressure, measurement of the time dependence of Q^{-1} after shutting the cell's valve showed this additional pressure to be negligible.

The oscillator's transfer function at low frequencies was measured in the bandwidths 0.008–3.1 Hz and 0.24–98 mHz. Overnight runs were required to obtain adequate signal-to-noise ratios at the lowest frequencies.

The oscillator's elastic aftereffect or creep was induced by quickly changing the dc bias voltage on one of the electrode pairs. The oscillator's position quickly changed by approximately 1 mrad, and during the next half hour it moved an additional few percent. During this creep measurement the lock-in's time constant was increased to either 0.4 or 4 s for an improved signal-to-noise-ratio.

Alternatives to anelasticity were tested. The gains of the lock-in amplifier and of the square root amplifiers were measured as a function of frequency. The accuracy of the spectrum analyzer was checked by measuring the transfer function of a resistive divider and a low-pass RC filter. The amplitude of the oscillator's drive was changed by a factor of 2. The balance of the capacitance bridge was moved from near 0 to half of the lock-in amplifier's full-scale output. The oscillator's transfer function was measured with both chirp and pure sine excitations. The results of these tests eliminated imperfect instrumentation as an explanation for the low-frequency behavior of the transfer function.

The nickel oscillator's creep was always consistent with the sign of the applied force. The creep could be induced by a step change in an external magnetic field as well as by the usual electric field, demonstrating the absence of uncontrolled electrostatic forces.

TABLE I. Q measured at 22 °C and β measured at T_β.

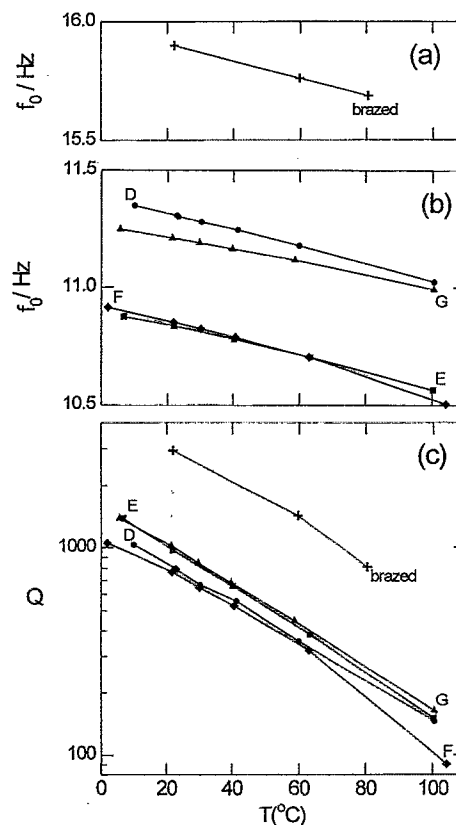| Oscillator	Q(22 °C)	β	T_β °C
D	820	0.174	61
E	970	0.198	63
F	770	0.195	63
G	1020	0.195	39
Brazed	2940	0.178	80

FIG. 3. (a), (b) The measured resonance frequencies f_0. (c) The quality factors Q. Although the brazed oscillator had losses which were lower than those of the Pb–Sn soldered oscillators, its temperature dependence was similar.

V. EXPERIMENTAL RESULTS

As shown in Fig. 3, the temperature dependences of ω_0 and Q^{-1} were similar for the four oscillators attached by the Pb–Sn solder. Almost all of the temperature dependence of ω_0 was caused by the temperature dependence of the shear modulus and not by the expansion coefficient of nickel. The large increase of Q^{-1} with temperature is not unusual, even for pure metals.[17,21] The value of Q at 90 °C is comparable to that measured by Rivière and Woirgard[21] in strain-hardened aluminum at a similar temperature and frequency $[\phi^{-1}(11 \text{ Hz}) \approx 200]$.

The losses Q^{-1} of the brazed oscillator were much smaller. One possible explanation for this difference is that large additional losses occurred in the Pb–Sn alloy. A second possible explanation is that the Pb–Sn contributed negligibly to Q^{-1}, and the brazed oscillator's Q^{-1} was decreased by its different thermal history, namely its much longer annealing time and the higher temperature used during torch brazing. In any case, the two types of oscillators had similar temperature dependences and, as shown in Table I, similar values for the exponent β.

Figure 4 plots oscillator F's displacement following a step change in the applied torque. After the initial, rapid change, the oscillator continued to creep an additional 4% during the next half hour. This creep could not be described by an exponential decay, but it was fitted well by Eq. (14)
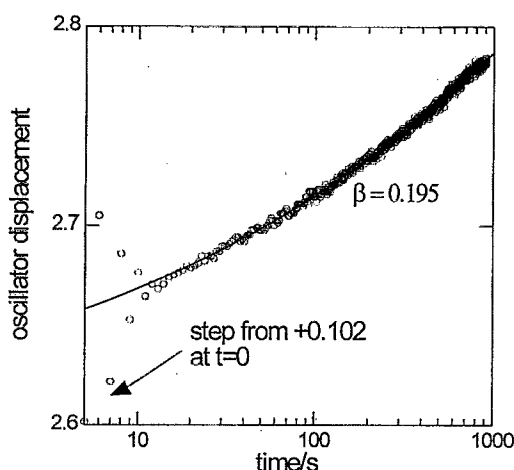
FIG. 4. The displacement, in arbitrary units, of oscillator F following a step change in the applied torque. The slow, nonexponential "elastic aftereffect" is made clear by use of the logarithmic time axis. Fitting Eq. (14) to these data yielded the exponent $\beta=0.195$.

with the two parameters β and the size of the initial jump. As shown in Table I, all five oscillators yielded $\beta=0.18$ to within 10%.

Figure 5 shows the frequency-dependent parts of the spring constant, extracted from the data by

$$\psi(\omega)+i\phi(\omega)=\frac{(k_{tr}/k_0)}{k_{tr}H(\omega)}-1+\left(\frac{\omega}{\omega_0}\right)^2,\qquad(16)$$
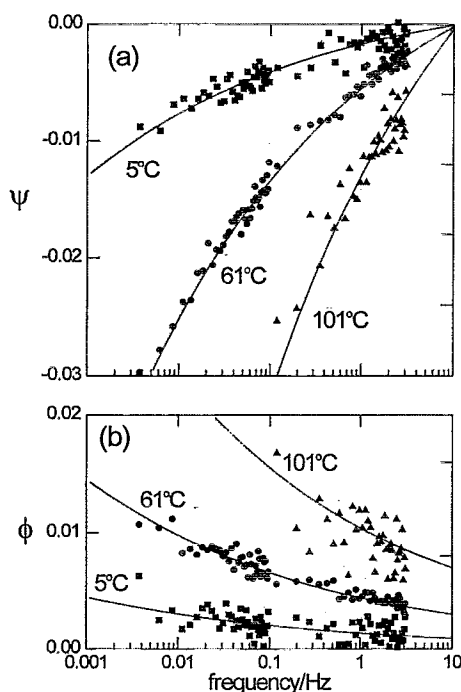

FIG. 5. (a) The real part $\psi(\omega)$ of the spring constant for oscillator D. Slight vertical shifts of the data, consistent with gain drift of the measuring electronics, were sometimes necessary to achieve consistency with the definition $\psi(\omega_0)\equiv0$. $(\omega_0/2\pi\approx11$ Hz.) The curves were calculated from Eq. (10) with no free parameters. (b) The imaginary part $\phi(\omega)$ of the spring constant. The curves were calculated from Eq. (3) with no free parameters.

where k_{tr} is a frequency-independent transducer constant. The values of $\phi(\omega)$ were thus derived from the measured function $k_{tr}H(\omega)$ and the measured numbers ω_0 and (k_{tr}/k_0). They were not sensitive to the value of (k_{tr}/k_0), which could be approximated by $|k_{tr}H(0.1$ Hz$)|$.

The values of $\psi(\omega)$ were sensitive to the estimate of (k_{tr}/k_0), and small adjustments for the difference $\mathrm{Re}[k(\omega_0)-k(0.1$ Hz$)]$ and for gain drift in the electronic instruments, were necessary to achieve consistency with the definition $\psi(\omega_0)\equiv0$. These adjustments merely shifted all of the values of $\psi(\omega)$ without changing the function's shape.

Superposed on the data for ψ and ϕ are curves from Eqs. (10) and (3). The parameters ω_0 and Q were fixed by the measurements at resonance, and the exponent β was fixed by the single measurement of creep at 61 °C. These curves describe the data over more than 3 decades of frequency below ω_0.

VI. DISCUSSION

To achieve accuracy over a wide range of frequencies, the model of a mechanical oscillator must include anelastic effects. In the absence of measurements far below ω_0, the simplest assumption is that the loss factor $\phi(\omega)$ is independent of frequency. However, because frequency dependence of $\phi(\omega)$ has been observed in a wide variety of materials, including pure metals, this assumption is too restrictive.

Equation (3) is an effective way to model weak frequency dependence of $\phi(\omega)$. It introduces only one additional parameter β, which is zero in the limit of constant ϕ. With the help of Eq. (14), a single measurement of the oscillator's creep is sufficient to determine both the applicability of Eq. (3) and the value of the exponent β. Equation (3) also leads to the simple Eq. (10) for the associated changes $\psi(\omega)$ in the spring's strength. Finally, as demonstrated by the present measurements, the temperature dependence of β can be weak, even when that of the quality factor Q is not.

ACKNOWLEDGMENTS

[1] C. Zener, *Elasticity and Anelasticity of Metals* (University of Chicago Press, Chicago, 1948).

[2] A. S. Nowick and B. S. Barry, *Anelastic Relaxation in Crystalline Solids* (Academic, New York, 1972).

[3] A. S. Nowick, in *Encyclopedia of Physics*, 2nd ed., edited by R. G. Lerner and G. L. Trigg (VCH, New York, 1991), p. 37.

[4] K. Bethe, D. Baumgarten, and J. Frank, Sensors Actuators A **21**, 844 (1990).

[5] T. J. Quinn, C. C. Speake, and L. M. Brown, Philos. Mag. A **65**, 261 (1992).

[6] P. R. Saulson, Phys. Rev. D **42**, 2437 (1990).

[7] A. Gillispie and F. Raab, Phys. Lett. A **190**, 213 (1994).

[8] A. Abramovici *et al.*, Science **256**, 325 (1992).

[9] R. F. Berg and M. R. Moldover, Science Requirements Document: Measurement of Viscosity Near the Liquid-Vapor Critical Point of Xenon, 1993.

[10] P. R. Saulson, R. T. Stebbins, F. D. Dumont, and S. E. Mock, Rev. Sci. Instrum. **65**, 182 (1994).

[11] *M3D: Mechanics and Mechanisms of Material Damping*, edited by V. K. Kinra and A. Wolfenden (STP 1169), (ASTM, Philadelphia, 1992).

[12] Proceedings of the Tenth International Conference on Internal Friction and Ultrasonic Friction in Solids [J. Alloys Compounds **211/212** (1994)].

[13] J. D. Ferry, *Viscoelastic Properties of Polymers* (Wiley, New York, 1980).

[14] J. Woirgard, Y. Sarrazin, and H. Chaumet, Rev. Sci. Instrum. **48**, 1322 (1977).

[15] P. Gadaud, B. Guisolan, A. Kulik, and R. Schaller, Rev. Sci. Instrum. **61**, 2761 (1990).

[16] G. D'Anna and W. Benoit, Rev. Sci. Instrum. **61**, 3821 (1990).

[17] G. D'Anna and W. Benoit, in Ref. 11, p. 358.

[18] A. Rivière and J. Woirgard, in Ref. 11, p. 525.

[19] O. Buck, O. N. Carlson, H. Indrawirawan, L. J. H. Brasche, and D. T. Peterson, in Ref. 11, p. 227.

[20] G. Schoeck, E. Bisogni, and J. Shyne, Acta Metall. **12**, 1466 (1964).

[21] A. Rivière and J. Woirgard, J. Alloys Compounds **211**, 144 (1994).

[22] P. Gadaud, A. Rivière, and J. Woirgard, in Ref. 11, p. 447.

[23] A. Lakki and R. Schaller, J. Alloys Compounds **211**, 365 (1994).

[24] Electroformed nickel mesh from Buckbee-Mears, St. Paul, MN 55101. In order to describe materials and experimental procedures adequately, it is occasionally necessary to identify commercial products by manufacturers' name or label. In no instance does such identification imply endorsement by the National Institute of Standards and Technology, nor does it imply that the particular product or equipment is necessarily the best available for the purpose.

[25] Hewlett–Packard model 35660A low-frequency spectrum analyzer.